

Functional Expression of an Arachnid Sodium Channel Reveals Residues Responsible for Tetrodotoxin Resistance in Invertebrate Sodium Channels*

Received for publication, July 16, 2009, and in revised form, September 9, 2009. Published, JBC Papers in Press, October 14, 2009, DOI 10.1074/jbc.M109.045690

Yuzhe Du, Yoshiko Nomura, Zhiqi Liu, Zachary Y. Huang, and Ke Dong¹

From the Department of Entomology, Genetics and Neuroscience Programs, Michigan State University, East Lansing, Michigan 48824

Tetrodotoxin (TTX) is a potent blocker of voltage-gated sodium channels, but not all sodium channels are equally sensitive to inhibition by TTX. The molecular basis of differential TTX sensitivity of mammalian sodium channels has been largely elucidated. In contrast, our knowledge about the sensitivity of invertebrate sodium channels to TTX remains poor, in part because of limited success in functional expression of these channels. In this study, we report the functional characterization in *Xenopus* oocytes of the first non-insect, invertebrate voltage-gated sodium channel from the varroa mite (*Varroa destructor*), an ecto-parasite of the honeybee. This arachnid sodium channel activates and inactivates rapidly with half-maximal activation at -18 mV and half-maximal fast inactivation at -29 mV. Interestingly, this arachnid channel showed surprising TTX resistance. TTX blocked this channel with an IC_{50} of $1 \mu\text{M}$. Subsequent site-directed mutagenesis revealed two residues, Thr-1674 and Ser-1967, in the pore-forming region of domains III and IV, respectively, which were responsible for the observed resistance to inhibition by TTX. Furthermore, sequence comparison and additional amino acid substitutions suggested that sequence polymorphisms at these two positions could be a widespread mechanism for modulating TTX sensitivity of sodium channels in diverse invertebrates.

Tetrodotoxin (TTX)² is a specific and potent blocker of voltage-gated sodium channels, which are essential for the initiation and propagation of action potentials in almost all excitable cells (1). TTX physically occludes the pore of sodium channels and blocks action potential conduction in nerve and muscle (1). The blocking effect of TTX on the sodium channel was first discovered in lobster giant axons (2). However, not all sodium channels are equally sensitive to TTX. For example, among the nine sodium channel isoforms ($rNa_v1.1$ to $rNa_v1.9$) from rats, TTX has high affinity for $rNa_v1.1$ – 1.4 , $rNa_v1.6$, and $rNa_v1.7$, blocking these channels (TTX-S) at nanomolar concentrations. In contrast, micromolar concentrations of TTX are required to block $rNa_v1.5$, $rNa_v1.8$, and $rNa_v1.9$, the TTX-resistant

(TTX-R) sodium channels (3, 4). In this regard, TTX is an effective pharmacological agent that has been used to distinguish different mammalian sodium channel isoforms.

The pore-forming α -subunit of mammalian voltage-gated sodium channels consists of four homologous domains (I–IV), each of which contains six transmembrane segments (S1–S6) and one reentrant P-region connecting S5–S6 (5) (Fig. 1A). In each P-region, the short segments, SS1 and SS2, span the membrane as a hairpin and form the lining of the transmembrane pore (5). Because TTX physically blocks the pore and prevents sodium conductance, elucidation of the TTX receptor site on sodium channels has been invaluable in elucidating the pore structure of sodium channels. In particular, site-directed mutagenesis of the SS1 and SS2 loops of domains I–IV revealed two motifs, DEKA (Asp-384, Glu-942, Lys-1422, and Ala-1714, located in domains I, II, III, and IV, respectively, of $rNa_v1.2$) and EEMD (Glu-387, Glu-945, Met-1425, and Asp-1717, located in domains I, II, III, and IV, respectively, of $rNa_v1.2$) as major determinants of the TTX receptor site (6, 7) (Fig. 1B). Predominantly negatively charged, the residues in the DEKA and EEMD motifs are equivalently positioned in each of the four domains. In combination, the DEKA and EEMD motifs form inner and outer rings of the sodium channel pore, respectively. The DEKA motif also forms the ion selectivity filter (8). Surprisingly, these two motifs are conserved in both TTX-sensitive and TTX-resistant sodium channels. Instead, a non-aromatic residue, cysteine or serine, immediately downstream of the first Glu in the EEMD motif of $rNa_v1.5$, $rNa_v1.8$, and $rNa_v1.9$ channels is responsible for TTX resistance (9–11).

In contrast to the presence of multiple sodium channel genes in vertebrates, invertebrates, such as jellyfish, flatworms, sea anemones, squid, mites, and insects, generally have fewer sodium channel-encoding genes (12). For example, only one sodium channel gene, *para*, is found in the fruit fly *Drosophila melanogaster* (13–16). Nevertheless, recent studies show that insects, such as *D. melanogaster* and the German cockroach (*Blattella germanica*), generate functional diversity of sodium channels by alternative splicing and RNA editing of a single sodium channel gene transcript (16–20). Characterization of more than 60 sodium channel variants from both *D. melanogaster* and *B. germanica* in *Xenopus* oocytes shows that all of these variants are highly sensitive to TTX (19, 20). TTX-insensitive sodium currents, however, have been reported in neurons of two jellyfish species (*Cyanea capillata* and *Polyorchis penicillatus*), which are the earliest extant organisms to incorporate

* This work was supported, in whole or in part, by National Institutes of Health Grant GM057440 and National Research Initiative of the United States Department of Agriculture Cooperative State Research, Education and Extension Service Grant 2004-35607-14866.

¹ To whom correspondence should be addressed. Tel.: 517-432-2034; Fax: 517-353-4354; E-mail: dongk@msu.edu.

² The abbreviations used are: TTX, tetrodotoxin; SS, short segment.

TTX Resistance in Invertebrate Sodium Channels

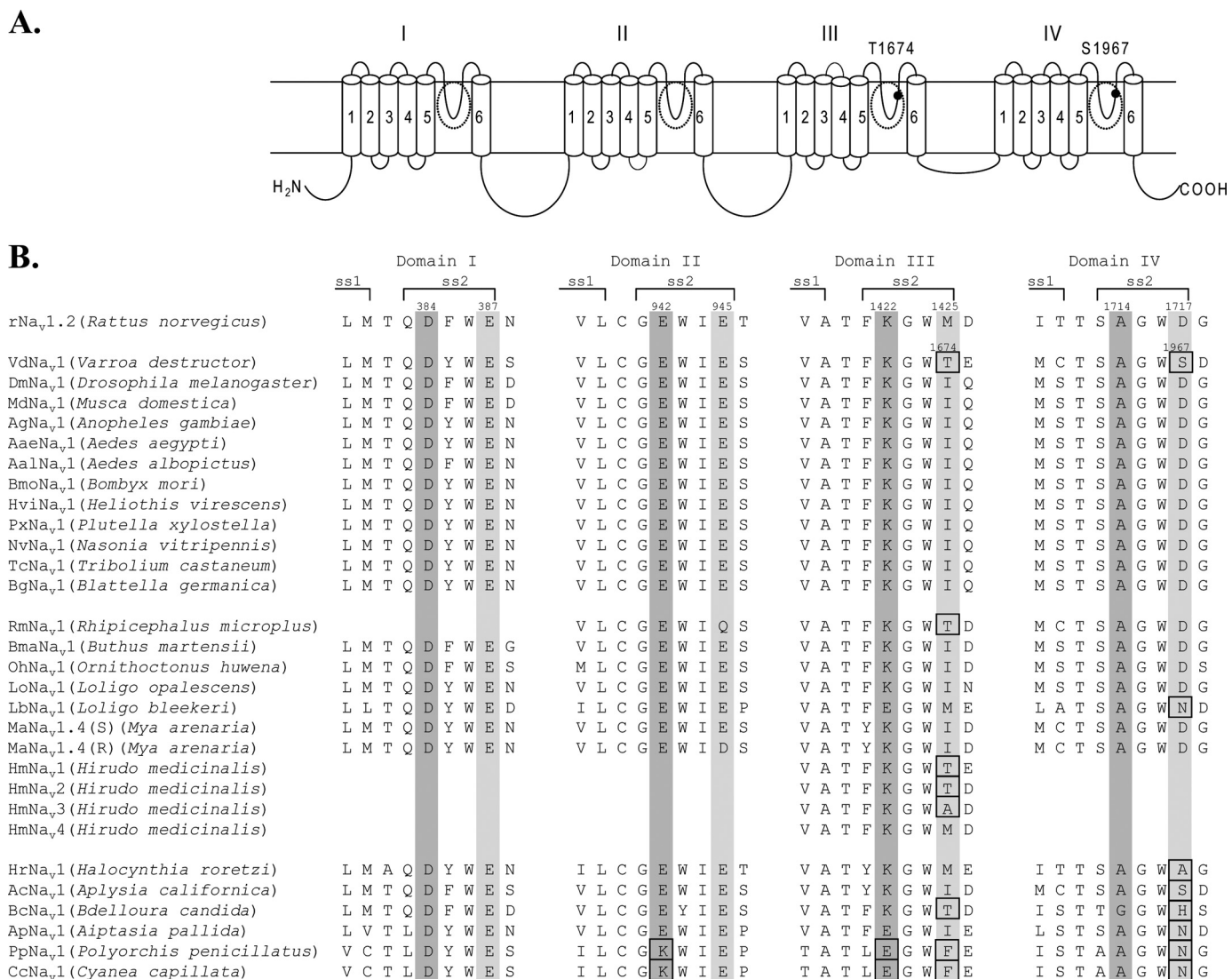


FIGURE 1. Sequence variations in the P-regions of sodium channels. A, A diagram of the topology of the α -subunit of voltage-gated sodium channels, which contain four homologous domains (I–IV), each consisting of six transmembrane segments. The short segments SS1 and SS2 in the P-region of each domain are indicated within a circle. The positions of two residues, Ser-1674 and Thr-1967, corresponding to Met-1425 and Asp-1717 in rNav1.2, are indicated. B, amino acid sequence alignment of SS1s and SS2s of all known invertebrate sodium channels. Only part of SS1 is shown. The DEKA and EEMD motifs are shaded. Residues deviating from the EEMD canonical motif are boxed. The *Rattus norvegicus* Na_v1.2 sodium channel (GenBank™ accession number, X03639) is included for comparison. Other sequences include: varroa mite *V. destructor* (AY259834), fruit fly *D. melanogaster* (M32078), house fly *Musca domestica* (X96668), African malaria mosquito *Anopheles gambiae* (AM422833), yellow fever mosquito *Aedes aegypti* (EU399179), Asian tiger mosquito *Aedes albopictus* (AY663384), domestic silkworm *Bombyx mori* (EU822499), tobacco budworm *Heliothis virescens* (AF072493), diamondback moth *Plutella xylostella* (BAF37093), jewel wasp *Nasonia vitripennis* (NM01134917), red flower beetle *Tribolium castaneum* (XM962937), German cockroach *B. germanica* (U73583), southern cattle tick *Rhipicephalus microplus* (AF134216), Manchurian scorpion *Buthus martensii* (AY322171), Chinese bird spider *Ornithoctonus huwena* (DQ839489), California market squid *Loligo opalescens* (L19979), spear squid *Loligo bleekeri* (D14525), TTX-sensitive and -resistant soft shell clam *Mya arenaria* (AAX14719), medicinal leech *H. medicinalis* (AY324424–AY324427), ascidian tunicate *H. roretzi* (D17311), California sea hare *A. californica* (U66915), turbellarian flatworm *B. candida* (U93074), sea anemone *Aiptasia pallida* (AF041851), hydrozoan jellyfish *P. penicillatus* (AF047380), and scyphozoan jellyfish *C. capillata* (L15445).

a nervous system (21–23). In addition, TTX-resistant sodium currents have also been detected in neurons of flatworms (*Bdelloura candida*) (24) and leeches (*Hirudo medicinalis*) (25). Alignment of the SS2 regions from sequenced invertebrate sodium channels reveals that the outer EEMD motif contains intriguing sequence polymorphisms in domains III and IV, but not in domains I and II (Fig. 1B). For instance, the residue corresponding to Met is a phenylalanine (Phe) in the two jellyfish sodium channels, and a threonine (Thr) in several other invertebrate sodium channels including flatworms and leeches (Fig. 1B). It is not known, however, whether the sequence polymor-

phisms in the EEMD motif of domains III and IV contribute to TTX insensitivity in invertebrate sodium channels.

To date, insect voltage-gated sodium channels are the only invertebrate sodium channels that have been functionally expressed in an *in vitro* expression system, despite reported attempts (26). Robust functional expression of insect sodium channels in *Xenopus* oocytes requires an accessory subunit, TipE (14). Therefore, it has been generally assumed that an unidentified accessory subunit like TipE may be required for functional expression of non-insect invertebrate sodium channels *in vitro* (26). Here, we report the functional expression and

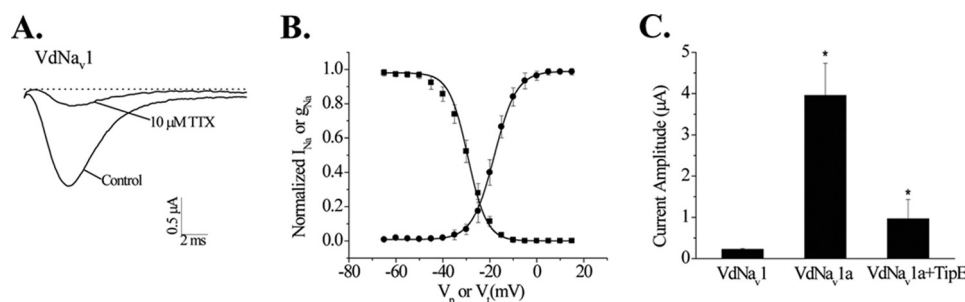


FIGURE 2. Functional characterization of VdNa_v1 in *Xenopus* oocytes. *A*, sodium current traces in the presence and absence of TTX. Sodium currents were generated with 20-ms depolarizations to -10 mV from a holding potential of -120 mV. *B*, voltage dependence of activation and inactivation. The voltage dependence of activation was measured by generating sodium currents with 20-ms depolarizations to potentials ranging from -80 to $+65$ mV in 5-mV increments from a holding potential of -120 mV. The voltage dependence of fast inactivation was determined using 100-ms conditioning prepulses to potentials ranging from -120 to 25 mV in 5-mV increments from a holding potential of -120 mV, followed by 20-ms test pulses to -10 mV. The voltage dependence of activation and steady-state inactivation curves were fitted with a Boltzmann equation. *C*, peak sodium currents of VdNa_v1 before (VdNa_v1) and after (VdNa_v1a) deletion of the exon B-like sequence and the effect of TipE on VdNa_v1a current amplitude. The amplitude of the peak current was measured during a 20-ms depolarization from -120 to -10 mV 4 days after cRNA injection. *, statistically significant difference compared with VdNa_v1; error bars represent S.D.

TABLE 1

Voltage dependence of activation and inactivation of wild-type and mutant sodium channels

The voltage dependences of conductance and inactivation were fitted with a two-state Boltzmann equation to determine $V_{1/2}$, the voltage for half-maximal conductance or inactivation, and k , the slope factor for conductance or inactivation. The values in the table represent the mean \pm S.D. and n is the number of oocytes used.

Na ⁺ channel type	Activation		Inactivation		<i>n</i>
	$V_{1/2}$	<i>k</i>	$V_{1/2}$	<i>k</i>	
	mV		mV		
VdNa _v 1	-18.23 ± 3.33	3.58 ± 0.57	-29.16 ± 1.72	4.98 ± 0.57	5
VdNa _v 1a	-19.78 ± 2.85	2.97 ± 0.69	-30.58 ± 2.08	4.47 ± 0.31	15
VdNa _v 1a + TipE	-20.34 ± 1.00	3.97 ± 0.31	-30.04 ± 1.41	4.52 ± 0.32	8

characterization of an arachnid sodium channel from the varroa mite (*Varroa destructor*), an ecto-parasite of the honeybee, in *Xenopus* oocytes. Interestingly, we found that this arachnid sodium channel is highly resistant to TTX. Site-directed mutagenesis enabled us to identify Thr-1674 and Ser-1967 as the molecular basis of TTX resistance of this sodium channel. Furthermore, sequence comparison and additional amino acid substitutions suggested that sequence polymorphisms in the EEMD motif of domains III and IV may be a widespread mechanism for modulating TTX resistance of sodium channels in invertebrates and possibly also in some vertebrates.

EXPERIMENTAL PROCEDURES

Isolation of a Full-length cDNA Clone by Reverse Transcription-PCR—We previously reported the cloning and sequencing of the coding region of a sodium channel (VdNa_v1; formerly called VmNa_v1) from the varroa mite (*V. destructor*) (27). To isolate a full-length cDNA clone for functional expression in *Xenopus* oocytes, the entire coding region was amplified by reverse transcription-PCR using total RNA isolated from a pool of about 1000 adult mites. The primers used in reverse transcription-PCR were oligo(dT)_{12–18}(RT), tagccggaattccgcaccatggcaccggcgcccgccgag (forward primer) and atgtgctctagattccacagcatcgctctgagc (reverse primer). The PCR product was cloned into pGH19, a *Xenopus* oocyte expression vector. A full-length clone was isolated and sequenced in the Research Technology Support Facility at Michigan State University.

Site-directed Mutagenesis—Site-directed mutagenesis was performed by PCR using appropriate mutant primers and Pfu Turbo DNA polymerase (Stratagene, La Jolla, CA). VdNa_v1a was generated by deleting a stretch of 24 nucleotides encoding VSIYYFST, homologous to exon B in a cockroach sodium channel, BgNa_v1-1a (19), using the same PCR mutagenesis method. All mutagenesis results were verified by DNA sequencing.

Functional Analysis in *Xenopus* Oocytes—Procedures for oocyte preparation and cRNA injection were identical to those described previously (28). The injected oocytes were incubated at 19 °C for 3–7 days before recording. The maximal peak

current was limited to <2.0 μ A to achieve better voltage control.

Methods for electrophysiological recording and data analysis were similar to those described previously (28, 29). The stock solution of TTX (1 mM) was dissolved in distilled water and working solutions were made in ND-96. The effect of TTX on sodium channel peak currents was measured 10 min after toxin application. Sodium currents were recorded by using a standard two-electrode voltage clamp technique. The voltage dependence of activation and fast inactivation were determined using protocols as described previously (28, 29). The data were fitted with a Boltzmann equation to generate $V_{1/2}$, the midpoint of the activation or inactivation curves, and k , the slope factor. Statistical significance was determined by Student's *t* test, and significant values were set at $p < 0.05$ or as indicated in the table and figure legends.

RESULTS

Functional Expression of the VdNa_v1 Channel in *Xenopus* Oocytes—Because there is no known accessory subunit identified in arachnids that is equivalent to β -subunits in mammals and TipE in insects, we attempted expression of the mite VdNa_v1 sodium channel alone by injecting cRNA of VdNa_v1 (10 ng/oocyte) into *Xenopus* oocytes. Sodium currents were detected 5–7 days after injection, even though the amplitude of peak current was small (less than 1 μ A after 7 days of cRNA injection). Nevertheless, the detected sodium currents were sufficient for functional characterization.

The VdNa_v1 channel activated and inactivated rapidly; a 20-ms depolarization to -10 mV from the holding potential of -120 mV almost completely inactivated the VdNa_v1 channel with a 5–10% non-inactivating current (Fig. 2A). The sodium channel exhibited steep voltage dependence of activation and fast inactivation (Fig. 2B). Interestingly, a significant overlap between the voltage dependence of activation and inactivation was observed (Fig. 2B and Table 1). At -26 mV, the crossing point of the two curves, about 20% of channels were not inacti-

TTX Resistance in Invertebrate Sodium Channels

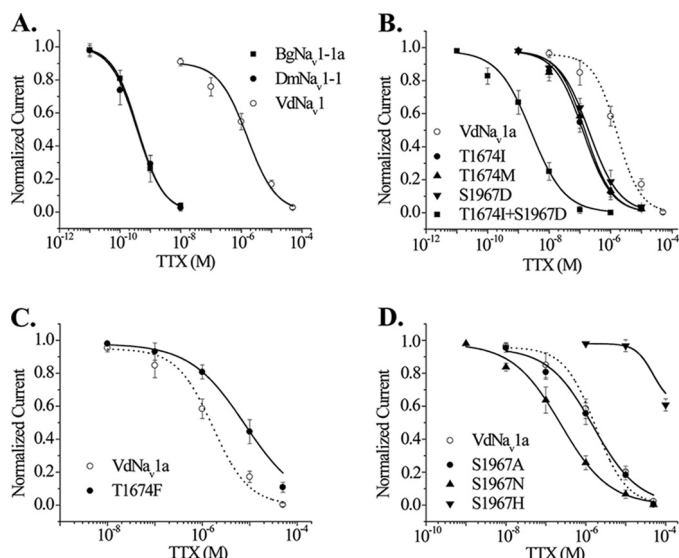


FIGURE 3. Distinct TTX sensitivities of wild-type and mutant sodium channels. *A*, dose-response curves of TTX inhibition for VdNa_v1 (open circle), BgNa_v1-1a (square), and DmNa_v1-1 (solid circle). *B*, dose-response curves of TTX inhibition for VdNa_v1a and the mutant channels, T1674I, T1674M, S1967D, and T1674I/S1967D. *C* and *D*, dose-response curves of TTX inhibition for VdNa_v1a and mutant channels carrying amino acid substitutions at domains III (*C*) and IV (*D*) found in other invertebrate sodium channels. Peak sodium currents elicited by a 20-ms depolarization to -10 mV from a holding potential of -120 mV were recorded 10 min after application of various concentrations of TTX. The amplitude of peak current in the presence of TTX was normalized to the amplitude of the peak current before the TTX treatment. Values are mean \pm S.D. (error bars). The curves were fitted with Langmuir isotherm to evaluate IC₅₀.

vated, indicating that these channels have the potential to produce window currents.

We previously showed that deletion of an optional exon, exon B, in the first linker connecting domains I and II of the cockroach sodium channel, BgNa_v1-1, greatly increased the amplitude of peak current (19). The sequence corresponding to exon B is present in VdNa_v1, although it is not known whether this exon-B-like sequence is also an optional exon in VdNa_v1. We deleted the exon-B-like sequence from VdNa_v1, creating the recombinant channel VdNa_v1a. As shown in Fig. 2C, deletion of the exon-B-like sequence greatly enhanced the peak current amplitude of VdNa_v1a by nearly 50-fold. However, it did not alter the channel gating properties (see Table 1). Furthermore, we co-expressed VdNa_v1a with the *D. melanogaster tipE* cRNA, which facilitates robust expression of insect sodium channels. Unexpectedly, addition of *tipE* cRNA reduced the expression of VdNa_v1a currents (Fig. 2C).

The VdNa_v1 Channel Is TTX Resistant—The concentration of TTX required to completely block the VdNa_v1 channel was 50 μ M, whereas 10 nM TTX was sufficient to block all current from the BgNa_v1-1a and the *Drosophila* sodium channel, DmNa_v1-1 (Fig. 3A). To determine the IC₅₀ of the VdNa_v1 channel to TTX, we generated a dose-response curve (Fig. 3A). VdNa_v1 channels are \sim 2,000-fold more resistant to TTX than the two insect sodium channels tested (Fig. 3A, Table 2). No difference was observed between VdNa_v1 and VdNa_v1a channels in response to TTX (Table 2). Because sodium current expression from VdNa_v1 was poor, and deletion of the exon B-like sequence did not affect the TTX activity and channel

TABLE 2
Sensitivity of wild-type and mutant sodium channels to TTX

Na ⁺ channel type	IC ₅₀ TTX	<i>n</i> ^a
	μ M	
VdNa _v 1	1.05 \pm 0.28	5
VdNa _v 1a	1.45 \pm 0.50	19
T1674I	0.12 \pm 0.03 ^b	10
T1674M	0.13 \pm 0.05 ^b	7
T1674F	6.95 \pm 2.89 ^b	6
S1967D	0.23 \pm 0.08 ^b	12
S1967N	0.21 \pm 0.06 ^b	11
S1967A	1.58 \pm 0.21	8
S1967H	>100 ^b	16
T1674I + S1967D	0.0027 ^b	10
BgNa _v 1-1a	0.0005 ^b	5
DmNa _v 1-1	0.0005 ^b	5

^a *n*, number of oocytes used.

^b Statistically significant difference compared with VdNa_v1a. The value represents the mean \pm S.D.

gating properties, we used VdNa_v1a for all subsequent experiments as presented below. We cannot rule out the possibility that deletion of the exon-B-like sequence has an unknown confounding effect with mutations in the pore-forming regions. However, the exon-B-like sequence is located in the second intracellular loop connecting domains II and III. The possibility of TTX sensitivity modulated by deletion of exon-B seems unlikely.

Identification of the Determinants of TTX Resistance of VdNa_v1—To elucidate the molecular basis of TTX resistance, we examined amino acid sequences of the P-regions, including TTX-interacting DEKA and EEMD motifs (see Fig. 1). The DEKA motif is conserved in the VdNa_v1 channel. However, the EEMD motif is not. Specifically, Met in domain III and Asp in domain IV are substituted with Thr and Ser, respectively. These two substitutions result in an EETS variant motif in the VdNa_v1 channel, instead of the canonical EEMD motif in mammalian sodium channels or the EEID variant motif in insect sodium channels (see Fig. 1).

To determine whether these two amino acid substitutions are responsible for TTX resistance of the VdNa_v channel, we replaced these residues with the corresponding residues in insect or mammalian sodium channels to produce three single mutation channels, T1674I (insect), T1674M (mammal), and S1967D (both insect and mammal), as well as a double mutant channel T1674I/S1967D. All three single substitutions significantly enhanced mutant channel sensitivity to TTX by about 10-fold (Table 2, Fig. 3B). Furthermore, the double mutant channel was about 400-fold more sensitive to TTX than the VdNa_v1a channel (Table 2, Fig. 3B). In fact, the level of TTX sensitivity of the double mutant channel is comparable with that of BgNa_v1-1a and DmNa_v1-1 (Table 2). These results provide strong evidence that substitution of the TTX-binding residues, methionine (isoleucine in insect sodium channels) and aspartic acid, in the mammalian EEMD motif with threonine and serine, respectively, renders the VdNa_v channel extremely resistant to TTX.

TTX Resistance Conferred by Substitutions with Residues Corresponding to Those in the EEMD Variant Motifs of Other Invertebrates—Like VdNa_v1, jellyfish (CcNa_v1) and flatworm (BcNa_v1) sodium channels possess sequence polymorphisms in the EEMD motif (Fig. 1). Specifically, the CcNa_v1 has a phenyl-

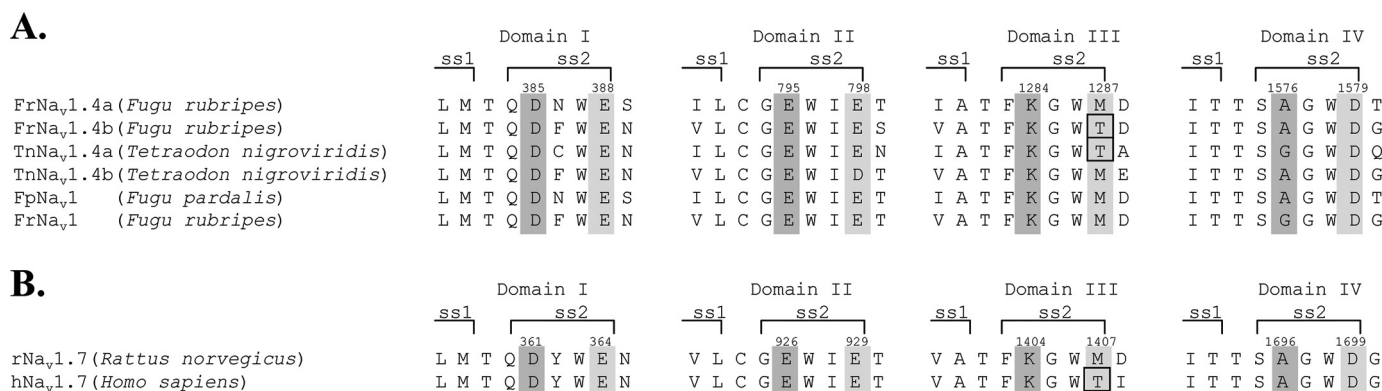


FIGURE 4. Amino acid alignment of the SS2s sequences of all four domains of pufferfish (A) and hNa_v1.7 (B) sodium channels. Sequences analyzed include two skeletal muscle sodium channels of tiger puffer *Fugu rubripes* (GenBank accession numbers ABB29441 and ABB29442), two skeletal muscle sodium channels of spotted green pufferfish *Tetraodon nigroviridis* (ABB29443 and ABB29444), panther puffer *Fugu pardalis* (AB030482), tiger puffer *Fugu rubripes* (D37977), and both *R. norvegicus* (AF000368) and human (X82835) Nav1.7 channel isoforms. The DEKA and EEMD motifs are shaded. The threonine substitutions of methionine in the EEMD motif in pufferfish and hNa_v1.7 sodium channel are boxed.

alanine residue instead of methionine in domain III and an asparagine residue instead of aspartic acid in domain IV, resulting in an EEFN variant motif. The flatworm BcNa_v1 channel also has a threonine in domain III as in VdNa_v, but a histidine residue instead of aspartic acid in domain IV, giving rise to an EETH variant motif. In addition, an alanine instead of an aspartic acid is found in an ascidian sodium channel (HrNa_v of *Holocynthia roretzi*) (30). Our experimental demonstration of TTX resistance in VdNa_v1a channels caused by sequence polymorphisms in the EEMD motif spurred our interest in examining the role in TTX sensitivity of the sequence polymorphisms identified in other invertebrate sodium channels.

The species-specific residues in the EEMD motif variants were introduced into VdNa_v1a channels by site-directed mutagenesis and the resultant mutant channels were examined for TTX sensitivity. The Thr to Phe substitution at position 1674 (T1674F), as identified in two jellyfish sodium channels, caused a 5-fold increase in TTX resistance compared with the VdNa_v1a channel (Fig. 3C, Table 2). The Ser to His substitution at position 1967 (S1967H), as present in the flatworm sodium channel, resulted in an extreme level of resistance to TTX. Only 40% of the peak current was inhibited by 100 μM TTX (Fig. 3D), the highest resistance observed in this study. The Ala substitution at position Ser-1967 (S1967A), as found in the ascidian sodium channel, did not alter TTX sensitivity of the VdNa_v1a channel (Fig. 3D). Finally, the Ser to Asn substitution at position 1967 (S1967N), as in jellyfish sodium channels, increased TTX sensitivity of the VdNa_v1a channel (Fig. 3D). Most of the amino acid substitutions used in these experiments reduced the amplitude of sodium current, but did not alter sodium channel gating properties (data not shown).

DISCUSSION

Prior to this study, insect sodium channels were the only invertebrate sodium channels that had been successfully expressed in *Xenopus* oocytes for functional characterization. Functional expression of insect sodium channels in *Xenopus* oocytes relies largely on co-expression of *tipE*, which encodes a small transmembrane accessory subunit protein (14). It is generally believed that the inability to functionally express other invertebrate sodium channels in *Xenopus* oocytes is likely

because an unknown accessory subunit that is functionally equivalent to TipE is required. Here, we successfully expressed a non-insect invertebrate sodium channel from the varroa mite in *Xenopus* oocytes. We found that functional expression of the VdNa_v1 sodium channel in *Xenopus* oocytes does not require co-expression of any accessory subunit. Surprisingly, co-expression of the *Drosophila* TipE with VdNa_v1 or VdNa_v1a reduced the amplitude of sodium currents. The possibility that varroa mites express an accessory protein *in vivo* capable of positively or negatively modulating VdNa_v expression cannot be ruled out.

Our analyses showed that VdNa_v1 sodium currents exhibited fast activation and inactivation kinetics that are typical of a voltage-gated sodium channel (Fig. 2A). This is not surprising considering that all essential sequences critical for sodium channel function are conserved in VdNa_v1, including the ion selectivity motif, the positively charged residues in S4 that form the voltage sensors, and the inactivation particle (27). A particularly striking feature of this channel is the apparent potential for window currents due to a significant overlap between the voltage dependence of activation and inactivation. Consequently, VdNa_v1 channels may generate a sustained sodium flux when the membrane potential is close to -26 mV. Similar window currents have been reported for the rNa_v1.9 channel (4) and several DmNa_v variants (20). In addition, the VdNa_v1 channel also exhibits a 5–10% non-inactivating current.

Although some invertebrates are well known to possess TTX-R sodium currents (21–25), the molecular bases of TTX resistance are not well understood. This lack of knowledge can be attributed largely to the inability to express invertebrate sodium channels in an *in vitro* system, such as *Xenopus* oocytes, for functional characterization. As discussed above, the only functionally characterized invertebrate sodium channels, prior to this study, are insect sodium channels (16, 31). However, no TTX-resistant insect sodium channels have been reported. The marked resistance of the VdNa_v1 channel to TTX therefore offers the first opportunity to investigate the molecular basis of TTX resistance in an invertebrate sodium channel. It appears that specific amino acid substitutions in domains III and IV of the EEMD motif represent a major route of evolution toward

TTX Resistance in Invertebrate Sodium Channels

TTX resistance in invertebrate species. In particular, a Thr or Phe substitution of Met in the EEMD motif is present in sodium channels from phylogenetically diverse invertebrates: jellyfish, flatworm, slug, leech, tick, and mite. Substitution of Asp with serine in the EEMD motif is found in sodium channels from the varroa mite and the sea slug (*Aplysia californica*), and an alanine substitution is found in ascidians (30). Although it remains to be further verified whether these substitutions affect TTX sensitivity of endogenous sodium channels from the respective invertebrate species, our functional assays using recombinant VdNa_v1a constructs strongly suggest that sodium channels from these invertebrate species possess various degrees of TTX resistance. Accordingly, characterization of molecular determinants of TTX resistance of the VdNa_v1a channel likely has uncovered a widespread mechanism for modulating TTX sensitivity in invertebrates.

Jellyfish are known to contain TTX-insensitive sodium currents (21–23). Our analysis of VdNa_v1a channels incorporating a methionine to phenylalanine substitution in the EEMD motif, as in jellyfish sodium channels, only reduced, but did not abolish, TTX sensitivity. The methionine to phenylalanine substitution does not entirely account for the TTX insensitivity of jellyfish sodium channels, however, suggesting that other amino acid changes or other mechanisms exist for TTX insensitivity. In mammalian sodium channels, the DEKA motif, which forms the selectivity filter, is also important for modulating TTX sensitivity (5). Neutralization of the Glu residue, charge reversal of Lys, or swapping of Glu and Lys in domains II and III in the DEKA motif renders the rNa_v1.2 channel extremely resistant to TTX (7, 32). Interestingly, two jellyfish sodium channels possess a DKEA motif, instead of the canonical DEKA motif (see Fig. 1). Therefore, it is possible that a combination of the unique DKEA motif and the methionine to phenylalanine substitution in the EEMD motif results in TTX insensitivity of sodium currents in these species.

Intriguingly, substitution of Met by Thr in the EEMD motif is also found in several vertebrate sodium channels including two pufferfish sodium channels, fuguNa_v1.4b and tetNa_v1.4a, and a human skeletal sodium channel, hNa_v1.7 (Fig. 4). Previous studies predicted that FuguNa_v1.4b channels would be TTX sensitive because these channels lack the previously identified TTX-resistant residues in domains I or II, which are found in fuguNa_v1.4a and tetNa_v1.4b (33). Our results suggest that fuguNa_v1.4b and tetNa_v1.4a sodium channels may be TTX resistant as well. The hNa_v1.7 channel may be TTX resistant, although rat rNa_v1.7 channels (the counterpart of hNa_v1.7) contain a canonical EEMD motif and have been shown to be TTX sensitive. In light of our findings, the TTX sensitivity of fuguNa_v1.4b, tetNa_v1.4a, and hNa_v1.7 need to be examined experimentally.

TTX, first isolated from pufferfish species, is found in animals of diverse taxa (34). The widespread detection of TTX-resistant sodium currents and sodium channels in phylogenetically diverse vertebrates and invertebrates suggests the biological and evolutionary importance of TTX resistance. For example, if TTX evolved as a chemical defense against potential predators, we could expect development of TTX resistance in organisms that feed on TTX-bearing food sources. Recent stud-

ies of sodium channels in garter snakes, which feed on TTX-bearing newts, illustrate such a scenario (34–36). Several species of newts were found to use TTX to defend against predacious garter snakes. As expected, certain populations of garter snakes that feed on TTX-possessing newts have developed TTX resistance as a result of mutations in the SS2 of domain IV in the outer pore of their skeletal muscle sodium channels (34, 35). Whereas attractive, the universality of this scenario remains to be determined in other species. Our identification and functional confirmation of additional amino acid substitutions in the EEMD motif associated with TTX resistance should facilitate future studies of potential evolutionary prey-predator relationships in diverse natural populations.

Acknowledgment—We thank Dr. Kris Silver for critical review of this manuscript.

REFERENCES

1. Hille, B. (1992) in *Ionic Channels of Excitable Membranes* (Hille, B., ed) pp. 59–82, Sinauer Associates, Inc., Sunderland, MA
2. Narahashi, T., Moore, J. W., and Scott, W. R. (1964) *J. Gen. Physiol.* **47**, 965–974
3. Goldin, A. L. (1999) *Ann. N. Y. Acad. Sci.* **868**, 38–50
4. Dib-Hajj, S., Black, J. A., Cummins, T. R., and Waxman, S. G. (2002) *Trends Neurosci.* **25**, 253–259
5. Catterall, W. A. (2000) *Neuron* **26**, 13–25
6. Noda, M., Suzuki, H., Numa, S., and Stühmer, W. A. (1989) *FEBS Lett.* **259**, 213–216
7. Terlau, H., Heinemann, S. H., Stühmer, W., Pusch, M., Conti, F., Imoto, K., and Numa, S. (1991) *FEBS Lett.* **293**, 93–96
8. Heinemann, S. H., Terlau, H., Stühmer, W., Imoto, K., and Numa, S. (1992) *Nature* **356**, 441–443
9. Satin, J., Kyle, J. W., Chen, M., Bell, P., Cribbs, L. L., Fozzard, H. A., and Rogart, R. B. (1992) *Science* **256**, 1202–1205
10. Sivilotti, L., Okuse, K., Akopian, A. N., Moss, S., and Wood, J. N. (1997) *FEBS Lett.* **409**, 49–52
11. Backx, P. H., Yue, D. T., Lawrence, J. H., Marban, E., and Tomaselli, G. F. (1992) *Science* **257**, 248–251
12. Goldin, A. L. (2002) *J. Exp. Biol.* **205**, 575–584
13. Loughney, K., Kreber, R., and Ganetzky, B. (1989) *Cell* **58**, 1143–1154
14. Feng, G., Deák, P., Chopra, M., and Hall, L. M. (1995) *Cell* **82**, 1001–1011
15. Zhou, W., Chung, I., Liu, Z., Goldin, A. L., and Dong, K. (2004) *Neuron* **42**, 101–112
16. Dong, K. (2007) *Invert. Neurosci.* **7**, 17–30
17. Tan, J., Liu, Z., Wang, R., Huang, Z. Y., Chen, A. C., Gurevitz, M., and Dong, K. (2005) *Mol. Pharmacol.* **67**, 513–522
18. Liu, Z., Song, W., and Dong, K. (2004) *Proc. Natl. Acad. Sci. U.S.A.* **101**, 11862–11867
19. Song, W., Liu, Z., Tan, J., Nomura, Y., and Dong, K. (2004) *J. Biol. Chem.* **279**, 32554–32561
20. Olson, R. O., Liu, Z., Nomura, Y., Song, W., and Dong, K. (2008) *Insect Biochem. Mol. Biol.* **38**, 604–610
21. Anderson, P. A. (1987) *J. Exp. Biol.* **133**, 231–248
22. Meech, R. W., and Mackie, G. O. (1993) *J. Neurophysiol.* **69**, 884–893
23. Spafford, J., Grigoriev, N., and Spencer, A. (1996) *J. Exp. Biol.* **199**, 941–948
24. Blair, K. L., and Anderson, P. A. (1993) *J. Exp. Biol.* **185**, 267–286
25. Kleinhaus, A. L., and Angstadt, J. D. (1995) *J. Neurobiol.* **27**, 419–433
26. Spafford, J. D., Spencer, A. N., and Gallin, W. J. (1998) *Biochem. Biophys. Res. Commun.* **244**, 772–780
27. Wang, R., Huang, Z. Y., and Dong, K. (2003) *Insect Biochem. Mol. Biol.* **33**, 733–739
28. Tan, J., Liu, Z., Tsai, T. D., Valles, S. M., Goldin, A. L., and Dong, K. (2002) *Insect Biochem. Mol. Biol.* **32**, 445–454

29. Tan, J., Liu, Z., Nomura, Y., Goldin, A. L., and Dong, K. (2002) *J. Neurosci.* **22**, 5300–5309
30. Nagahora, H., Okada, T., Yahagi, N., Chong, J. A., Mandel, G., and Okamura, Y. (2000) *Biochem. Biophys. Res. Commun.* **275**, 558–564
31. Soderlund, D. M. (2006) in *Sodium Channel, Comprehensive Molecular Insect Science: Pharmacology* (Lawrence, G., Kostas, I., and Gillo, S., eds) Vol. 5, pp. 1–24, Elsevier Science Publishers, New York
32. Schlieff, T., Schönherr, R., Imoto, K., and Heinemann, S. H. (1996) *Eur. Biophys. J.* **25**, 75–91
33. Venkatesh, B., Lu, S. Q., Dandona, N., See, S. L., Brenner, S., and Soong, T. W. (2005) *Curr. Biol.* **15**, 2069–2072
34. Soong, T. W., and Venkatesh, B. (2006) *Trends Genet.* **22**, 621–626
35. Geffeney, S., Brodie, E. D., Jr., Ruben, P. C., and Brodie, E. D., 3rd (2002) *Science* **297**, 1336–1339
36. Geffeney, S. L., Fujimoto, E., Brodie, E. D., 3rd, Brodie, E. D., Jr., and Ruben, P. C. (2005) *Nature* **434**, 759–763